The "Realstruktur" of the System $La_{2-x}Sr_xCu_{1-y}Ru_yO_{4-\delta}$ Studied by Rietveld and Extended X-ray Absorption Fine Structure Spectroscopy†

Stefan Ebbinghaus, Michael Fröba, and Armin Reller*

Institute of Inorganic and Applied Chemistry, University of Hamburg, Martin-Luther-King-Platz 6, D-20146 Hamburg, Germany

Received: May 8, 1997[⊗]

The structure of the layered perovskite-related system $La_{2-x}Sr_xCu_{1-y}Ru_yO_{4-\delta}$ was investigated by Rietveld refinement calculations of X-ray diffraction data and EXAFS analysis of the Ru−K and Cu−K absorption edge. Both methods complement one another as they yield information about long-range ordering and the local environment of a specific element, respectively. Rietveld calculations have revealed remarkable changes of the interatomic distances with the composition, e.g., the degree of elongation of the Cu/Ru−O_6 octahedra. To get more detailed information about the local structure we have performed EXAFS studies for selected samples with $y = 0$, 0.2, 0.4, 0.6, 0.8, and 1. We were able to achieve consistent results both from the Ru−K and Cu−K edge data. As an element specific method, extended X-ray absorption fine structure (EXAFS) spectroscopy is capable of distinguishing between different possible arrangements of the La/Sr and Cu/Ru atoms. We found that La and Sr are distributed statistically on the A cation position. For the B cations a small enrichment of Cu in the Ru surrounding (and vice versa) could be detected. For a given value of y this enrichment increases with increasing La content. This indicates a partial ordering of Ru and Cu within the perovskite layers. Oxygen vacancies ($\delta > 0$) were found to be located exclusively in the Cu surrounding. Coordination numbers less than 5 reveal that a part of the copper ions is coordinated in a square planar way. Distances derived from EXAFS and XRD data show a good agreement; still, the former are usually smaller by 0.01−0.03 Å. The distance Cu−La/Sr was found to be smaller by 0.05 Å than the distance Ru−La/Sr. Apart from this, no significant differences could be detected for the distances between the various combinations of elements.

Introduction

The atomic and electronic structure of perovskite-related metal oxides may be fine tuned by metal cation substitution as well as by oxygen stoichiometry alteration. In turn, these possibilities allow the tailoring of physical and chemical properties. Therefore perovskite-related metal oxides prove to be the functional materials of many noteworthy technologies. To really understand composition−structure−property relations or—even more demanding—dynamic processes, such as electronic or ionic conductivity, it is necessary to not only determine average structures and average bulk properties but also the local moieties and their relative arrangements, as well as their interactions in the structural framework. Consequently, local probes, such as extended X-ray absorption fine structure (EXAFS) spectroscopy or other spectroscopic methods, are the useful tool to complement conventional methods such as X-ray diffraction or electron microscopy. As is shown in this study, the combination of local and averaging probes may yield considerably more detailed insight into the "Realstruktur" of functional solids (Note: Up to now the term "Realstruktur" did not find an adequate translation in English. It is, however, the *terminus technicus* for the description of a solid with its individual compositional, structural, and morphological features).

Recently we have reported the synthesis and characterization of about 90 members of the system $La_{2-x}Sr_xCu_{1-y}Ru_yO_{4-\delta}$.[1]

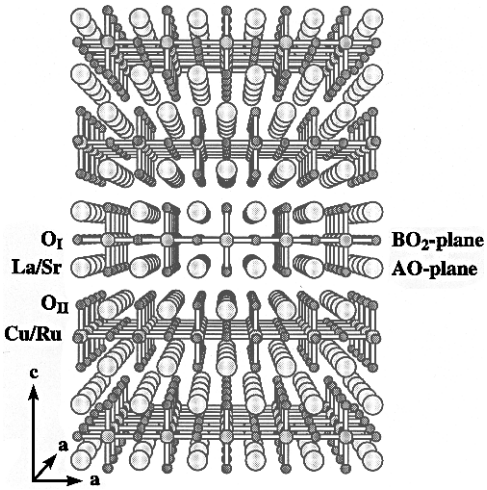

Figure 1. Structure of $La_{2-x}Sr_xCu_{1-y}Ru_yO_{4-\delta}$.

We were able to synthesize single phase samples in the entire range of $0 \le y \le 1$ with $x \ge 2y$. All samples adopt the K_2NiF_4 type structure (Figure 1). Preparation was done by conventional solid-state reactions. Starting materials were RuO_2, CuO, La_2O_3, and $SrCO_3$.

The system exhibits some interesting structural properties. Both cell parameters a and c show a complex dependence on the values of x and y with several local maxima and minima. Rietveld calculations have revealed some remarkable changes in the atomic distances as a function of the composition. As an example, it was found that a decrease of the lattice parameter c leads to an approach of the neighboring AO layers in the K_2NiF_4 structure while the distance between these rock salt type layers and the BO_2 planes remains almost unchanged.

* Corresponding author. Institute of Inorganic and Applied Chemistry, University of Hamburg, Martin-Luther-King-Platz 6, D-20146 Hamburg, Germany. Fax: ++49 40 4123 6348. Phone: ++49 40 4123 3103. E-mail: reller@xray.chemie.uni-hamburg.de.

† This work is dedicated to Prof. Sir John Meurig Thomas on the occasion of his 65th birthday.

⊗ Abstract published in *Advance ACS Abstracts,* November 1, 1997.

S1089-5647(97)01551-4 CCC: $14.00

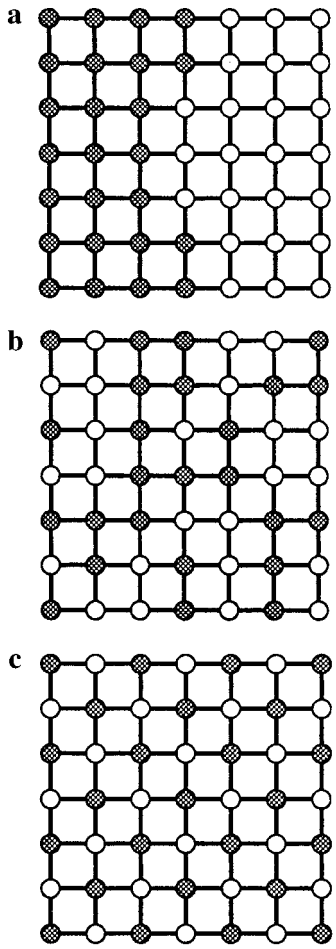

Figure 2. Three possible arrangements of B cations within a single BO_2 layer (oxygen atoms have been omitted). (a) Ordered arrangement in which Ru (Cu) is surrounded predominantly by Ru (Cu). (b) Random distribution: Ru (Cu) is surrounded both by Ru and Cu. (c) Chessboard-like arrangement in which Ru is surrounded exclusively by Cu and vice versa.

To determine the oxygen content of our samples, we have performed thermogravimetric measurements. From the weight loss during reduction in hydrogen atmosphere we found that the substitution of La^{3+} by Sr^{2+} leads to a formation of up to 40% of Cu^{III} or Ru^{V}. If the Sr content is further raised, the system reacts with the loss of oxygen which finally leads to a breakdown of the K_2NiF_4 structure and the formation of impurity phases. The oxygen deficit can roughly be approximated by the following formula

$$\delta \approx 0 \qquad \text{for} \qquad x \leq 2y + 0.4$$

$$\delta \approx \frac{x}{2} - y - 0.2 \qquad \text{for} \qquad x > 2y + 0.4$$

In the course of our research the question arose whether the different atomic species (La, Sr and Cu, Ru) are distributed statistically on the A and B cation positions or whether short range orderings occur. As an example, Figure 2 shows three possible arrangements within one BO_2 plane (for clearness the oxygen atoms have been omitted): Figure 2a shows an ordered arrangement in which copper and ruthenium are predominantly surrounded by B cations of the same kind. Figure 2b shows a statistical distribution while Figure 2c displays an ordered (chessboard-like) arrangement in which Cu is surrounded exclusively by Ru and vice versa. Note that for all three possibilities the ratio Cu:Ru is the same (1:1).

Another question that arose was whether the thermogravimetrically determined oxygen vacancies are located in the surrounding of only one B cation species (Cu or Ru) or whether both of them are affected by the loss of oxygen.

Finally we were interested to find out whether the distances between different combinations of atoms are equal, that is whether $d(\text{Cu}-\text{La}) = d(\text{Cu}-\text{Sr}) = d(\text{Ru}-\text{La}) = d(\text{Ru}-\text{Sr})$ and $d(\text{Cu}-\text{Cu}) = d(\text{Cu}-\text{Ru}) = d(\text{Ru}-\text{Ru})$.

Diffraction studies are inadequate to answer these questions as they can only give average structural information. EXAFS, on the other hand, yields information about the local environment of a specific element, and therefore, it should be perfectly suited for this kind of problems.

Experimental Section

We have performed EXAFS investigations both at the Cu−K edge and the Ru−K edge for a series of selected samples with $y = 0$, 0.2, 0.4, 0.6, 0.8, and 1.

About 60 mg of the oxide and 30 mg of polyethylene were thoroughly mixed and pressed to pellets of 13 mm diameter.

Measurements were carried out on the beamlines E4 (Cu) and X1.1 (Ru) at HASYLAB at DESY, equipped with Si(111) and Si(311) double-crystal monochromators, respectively.

The samples were measured in transmission mode at room temperature (Cu) and 77 K (Ru). All spectra were recorded using a continuous scan technique (QEXAFS).[2]

The counting time per data point was 0.6 s for Cu (Ru, 0.8 s); the step width was 2.5 eV both for Cu and Ru. The spectra were calibrated against the first inflection point of the K-edge of the corresponding metal (Cu, 8.979 keV; Ru, 22.117 keV), which was measured simultaneously.

For the evaluation of the EXAFS data, the program WinXAS[3] was used. The preedges were normalized for absorbance by fitting the spectral region from 8.7 to 8.9 keV (Ru, 21.9−22.05 keV) with a Victoreen function and subtracting this as background absorption. In addition, all spectra were normalized for atomic absorption by using the average absorption coefficient of the region from 9.03 to 9.16 keV (Ru, 22.19−22.37 keV). The photon energy E to wave vector k conversion was carried out using the first inflection point of the absorption edge as energy threshold. The atomic absorption μ_0 was subtracted by fitting the k^3-weighted spectra in the range $3 \leq k \leq 14$ Å^{-1} ($3.5 \leq k \leq 17$ Å^{-1} for Ru) with a seventh-degree polynomial function. For the Fourier transformation, the same data region was weighted with a Bessel Window ($\beta = 4$).

Theoretical scattering phase shifts and amplitudes were calculated using FEFF6.01.[4]

X-ray diffraction data were collected on a Philips XPERT diffractometer using Cu Kα radiation. The step size was 0.02° 2θ, and the counting time was 1 s/data point.

For Rietveld refinement calculations the program DBWS-9411 was used.[5] The background was approximated by a linear intrapolation between 30 data points in regions where no Bragg reflections were present. For the peak shape a pseudo-Voigt profile function was applied.

Results and Discussion

For most of the Rietveld calculations, agreement between observed and calculated intensities was quite good with residual values $R_p < 8$ and $R_{wp} < 10$. A typical Rietveld diagram is shown in Figure 3. In Table 1 the lattice parameters and fractional coordinates for the system $La_{2-x}Sr_xCu_{1-y}Ru_yO_{4-\delta}$ are listed. Table 2 shows the corresponding distances between the central Cu/Ru ion and all atoms within a sphere of 5 Å radius. It can be seen that the distances can be determined with an

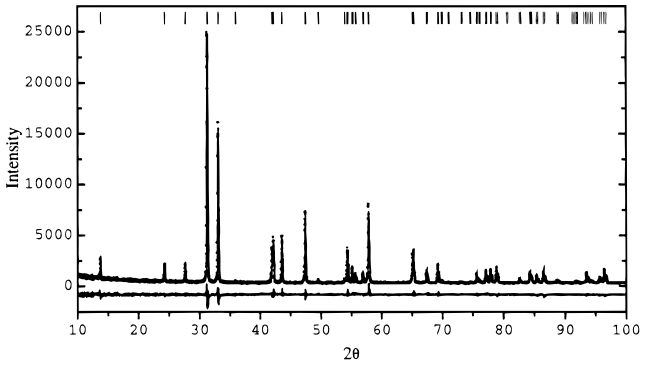

Figure 3. Typical Rietveld refinement plot. Observed (dots), calculated (line), and difference (bottom line) intensities. The markers indicate the calculated peak positions.

accuracy better than 0.01 Å for O_{II} and 0.002 Å for all other atoms. These results are in good accordance with the ones reported earlier.[1]

The distances obtained by XAS spectroscopy will be compared with those obtained by Rietveld calculations in the following.

Figures 4a and 5a show the extracted $\chi(k)k^3$ of the Ru−K and Cu−K edge for three samples with $y = 0.6$ and different Sr content. In Figures 4b and 5b the corresponding Fourier transforms are shown. The modified radial distribution functions (RDF) show four main peaks below $R = 4.5$ Å. These peaks lie roughly at 1.5, 2.6−3.0, 3.4−3.7, and 4.2 Å.

By comparing these values with the ones listed in Table 2, the four main peaks can be associated to the distances Cu/Ru−O_I/O_{II}, Cu/Ru−La/Sr($^1/_2,^1/_2,^1/_2 - z$), Cu/Ru−Cu/Ru(1,0,0), and Cu/Ru−La/Sr(0,0,z), respectively.

Looking at the oxygen shell it is striking that x barely affects the ruthenium coordination, while the Cu−O peak decreases considerably with increasing Sr content (Figures 4b and 5b).

This already indicates, in a qualitative way, that the oxygen vacancies are located exclusively in the copper surrounding.

Considering the first La/Sr shell, one finds that an increasing Sr content leads to an increasing peak height both for the Cu−K and Ru−K EXAFS. At the same time, the peaks are shifted toward larger distances.

The Cu/Ru peaks behave contrarily in the Ru and Cu EXAFS. For the former this peak increases with increasing Sr content and is shifted toward smaller R values, while for the latter its behavior is just vice versa.

The second La/Sr peak is rather small in the RDFs displayed in Figure 4b and 5b. Nevertheless, this peak was much better pronounced for other samples (see, for example, Figure 7b).

For a quantitative analysis the modified radial distribution functions were fitted using theoretical phase shifts and amplitudes calculated with the program FEFF6.01.[4]

The atomic positions for the input files were generated from the results listed in Table 1. The keep criteria for the plane wave and curved wave amplitude filters were set to 5% and 10%, respectively. The significance of each path found by FEFF was checked by simulating its $\chi(k)$ and RDF. We found when, for $R \geq 5$ Å, the number of possible paths (including numerous multiple scattering paths) gets that large a meaningful data analysis becomes impossible. So we have restricted our efforts to the four main peaks described above. The most important scattering paths are shown in Figure 6. For the first two shells, which consist of the oxygen octahedra and a cube of 8 La/Sr ions around the central Cu/Ru atom, only single scattering paths were found. For the third peak three possible paths were detected: the direct Cu/Ru−Cu/Ru(1,0,0) backscattering and two multiple scattering paths, namely, Cu/Ru−O($^1/_2$,0,0)−Cu/Ru(1,0,0) and Cu/Ru−O($^1/_2$,0,0)−Cu/Ru(1,0,0)−O($^1/_2$,0,0). It turned out that the amplitude of the direct scattering path was much smaller than the amplitudes of the multiple scattering paths. For the Cu/Ru−O−Cu/Ru−O path, on the other hand, the calculated phase shift was found to be wrong. When trying to fit the experimental RDFs with the data for this path we found unreliable distances and values for E_0 of about −60 eV.

For this reason and in order to reduce the number of free variables only the Cu/Ru−O−Cu/Ru scattering path was considered during the fits.

A similar situation was found for the La/Sr(0,0,z) peak. Again the multiple scattering path Cu/Ru−O(0,0,z)−La/Sr(0,0,z) was much more intense than the direct path so the former could be neglected.

Finally we found that for the Ru−K EXAFS the quality of the fit was much improved when the scattering path Cu/Ru−O(1,$^1/_2$,0) was included. For a better stability of the least-squares refinement runs, the distance for this path was fixed to $(5/4)^{1/2}a$. (Note: Actually there are two different distances: $(5/4)^{1/2}a$ and $(a^2 + (z_{O_{II}}c)^2)^{1/2}$ (Table 2). But as these are quite similar we have fixed all atoms at the former distance.)

It is well-known that the values for S_0^2, N, and σ are highly correlated.[6] For this reason, a simultaneous refinement of all three parameters will most likely lead to incorrect results. As we were predominantly interested in the determination of the coordination numbers we first had to find reliable values for S_0^2 and σ. Therefore, we have started our calculations with Sr_2RuO_4 as a reference material. The coordination numbers were fixed to their known values and S_0^2, σ, and E_0 were refined. The oxygen shell and the four other shells were fitted in two different runs. Results can be found in Table 3. The fit was repeated with a second data set in order to check whether the results are reproducible. Both fits yielded the same values within the errors given in the table.

The values of S_0^2, σ, and E_0 were fixed for the other compounds where we made the assumption that La and Cu possess the same Debye−Waller factors as Sr and Ru. The coordination numbers for the different atoms were correlated in the way that their sum was set equal to the degeneracy of the corresponding path, e.g., $N(\mathrm{La}) + N(\mathrm{Sr}) = 8$. The distances for La and Sr at(0,0,z) were also correlated during the fit in order to achieve stable results.

Figure 7a displays the experimental Ru−K $\chi(k)k^3$ for the sample $La_{0.2}Sr_{1.8}Cu_{0.2}Ru_{0.8}O_{4-\delta}$ and its simulation. In Figure 7b the corresponding Fourier transforms are shown. The good agreement of the fit is evident. Finally Figure 7c shows the contributions of the different atom species.

The fit results for all compounds are listed in Table 3.

Looking at the Ru−oxygen shell it can be seen that the coordination number for all samples is 6 within a range of ±0.3. This clearly proves that Ru remains in an octahedral coordination sphere independent of the oxygen content of the sample.

From the Rietveld refinements of the X-ray diffraction (XRD) data it is known that this shell is not an ideal octahedron but rather an elongated tetragonal bipyramid. We have tried to fit the X-ray absorption (XAS) data with two separate oxygen shells, but this did not lead to reliable results. It turned out that the choice of the R range used for the fit had a strong influence on the result. Furthermore, the errors for the distances were quite large (about 0.2 Å). For these reasons we have decided to use only one oxygen shell for the fit. The distances of this shell were almost the same for all samples (1.93 ± 0.01 Å). Compared with the averaged O_I/O_{II} distances derived from

TABLE 1: Cell Parameters, Atomic Positions, and Final *R* Values for the Rietveld Refinement Calculations of the System $La_{2-x}Sr_xCu_{1-y}Ru_yO_{4-\delta}$

x	y	a (Å)	c (Å)	$z_{(O_{II})}/c$	$z_{(La,Sr)}/c$	R_p	R_{wp}
2	1	3.8724 (3)	12.7423 (10)	0.1625 (5)	0.3527 (1)	6.95	9.90
1.8	0.8	3.9018 (3)	12.6264 (3)	0.1649 (5)	0.3541 (1)	7.37	10.36
1.92	0.6	3.9140 (1)	12.5266 (5)	0.1602 (4)	0.3562 (1)	7.00	9.30
1.6	0.6	3.9097 (1)	12.6295 (4)	0.1661 (4)	0.3566 (1)	7.13	9.30
1.36	0.6	3.8784 (3)	12.8086 (14)	0.1686 (7)	0.3561 (1)	7.74	10.39
1.4	0.4	3.8692 (1)	12.7798 (5)	0.1672 (7)	0.3566 (1)	7.19	9.66
1.2	0.2	3.8212 (1)	12.8778 (6)	0.1673 (4)	0.3579 (1)	6.87	8.74
0.1	0	3.7838 (1)	13.2302 (4)	0.1827 (4)	0.3607 (1)	8.26	10.37

TABLE 2: Distances between the Cu/Ru (0,0,0) Ion and All Atoms within a Sphere of 5 Å Radius

atom	$x = 2$ and $y = 1$ distance (Å)	$x = 1.8$ and $y = 0.8$ distance (Å)	$x = 1.92$ and $y = 0.6$ distance (Å)	$x = 1.6$ and $y = 0.6$ distance (Å)	$x = 1.36$ and $y = 0.6$ distance (Å)	$x = 1.4$ and $y = 0.4$ distance (Å)	$x = 1.2$ and $y = 0.2$ distance (Å)	$x = 0.1$ and $y = 0$ distance (Å)
$O_I(1/2,0,0)$	1.9362 (2)	1.9509 (2)	1.9570 (1)	1.9548 (1)	1.9392 (2)	1.9346 (1)	1.9106 (1)	1.8919 (1)
$O_{II}(0,0,z)$	2.071 (6)	2.082 (6)	2.007 (5)	2.098 (5)	2.160 (9)	2.137 (9)	2.154 (5)	2.417 (5)
La/Sr$(1/2,1/2,1/2 - z)$	3.320 (1)	3.317 (1)	3.302 (1)	3.305 (1)	3.304 (1)	3.293 (1)	3.263 (1)	3.249 (1)
Cu/Ru(1,0,0)	3.8724 (3)	3.9018 (3)	3.9140 (1)	3.9097 (1)	3.8784 (3)	3.8692 (1)	3.8212 (1)	3.7838 (1)
$O_I(1,1/2,0)$	4.3295 (3)	4.3623 (3)	4.3760 (1)	4.3712 (1)	4.3362 (3)	4.3259 (1)	4.2722 (1)	4.2304 (1)
$O_{II}(1,0,z)$	4.391 (4)	4.423 (4)	4.398 (3)	4.437 (3)	4.439 (5)	4.420 (5)	4.387 (4)	4.490 (4)
La/Sr(0,0,z)	4.494 (1)	4.471 (1)	4.462 (1)	4.504 (1)	4.561 (1)	4.557 (1)	4.609 (1)	4.772 (1)

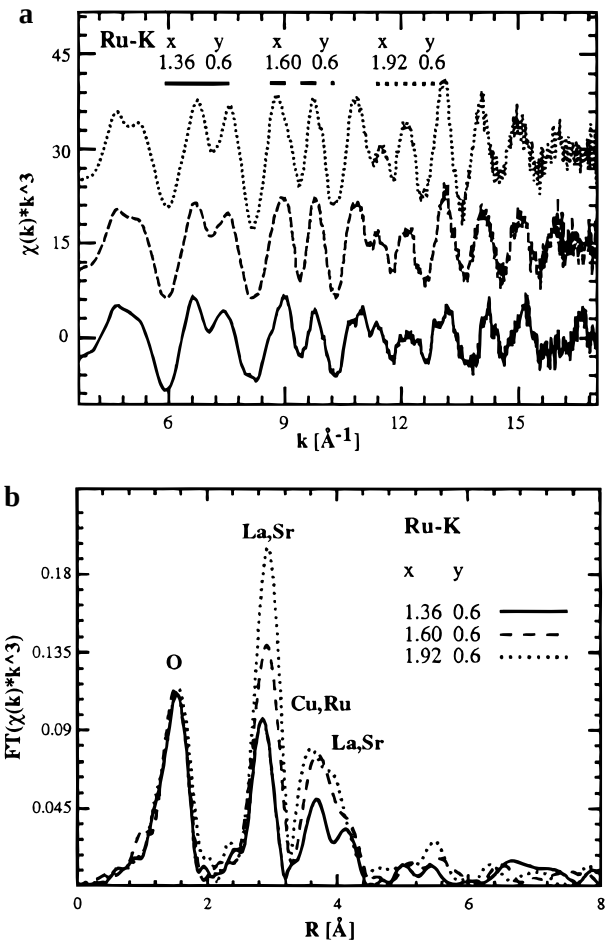

Figure 4. (a) Extracted $\chi(k)k^3$ for the Ru−K edge EXAFS of three samples with $y = 0.6$. (b) Modulus of the Fourier transforms of the Ru−K $\chi(k)k^3$.

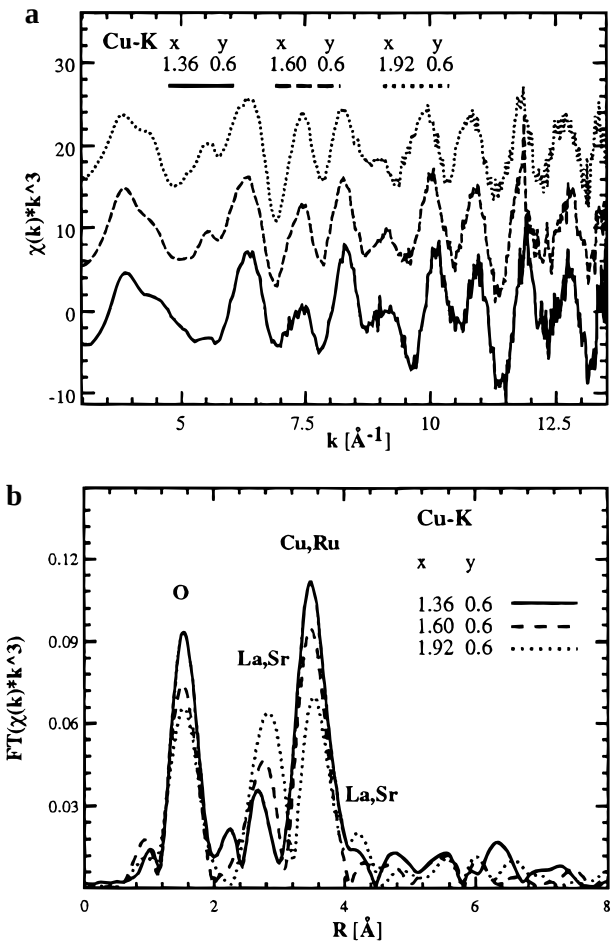

Figure 5. (a) Extracted $\chi(k)k^3$ for the Cu−K edge EXAFS of the same samples as shown in Figure 4a. (b) Modulus of the Fourier transforms of the Cu−K $\chi(k)k^3$.

Rietveld refinements (1.97−2.01 Å), this value is a little bit too small.

Considering the first La/Sr peak, it can be seen that the value of R is nearly equal for all samples with $y > 0.2$ (3.29 ± 0.01 Å). Again the XRD distances (3.29−3.32 Å) are larger. It is noteworthy that the distance Ru−La is the same as the distance Ru−Sr. (Note that both distances were used as independent fitting parameters.)

The coordination numbers for La and Sr are in good agreement with the ones expected for a statistical distribution of the A cations. The deviation is less than 0.4 for all samples except $x = 1.92$ and $y = 0.6$.

It was already mentioned that for $y = 0.6$ the La/Sr peak decreases and is shifted to smaller R values as the La content is increased. Nevertheless, the distances obtained by the least squares algorithm are equal for all three compounds. We found

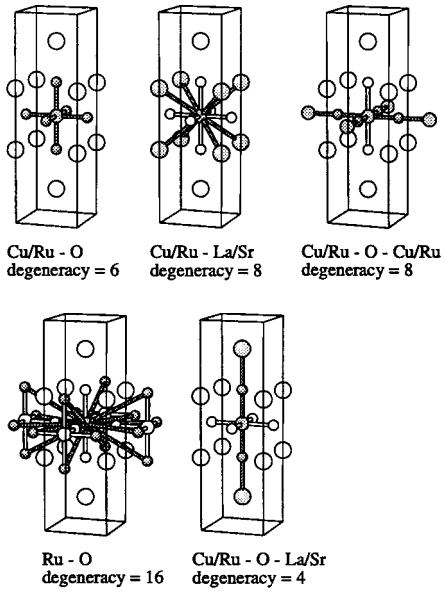

Figure 6. Main scattering paths. The shaded atoms are the ones involved in the path.

that both increasing and shifting of the peak are due to a negative interference of the backscattering contributions of La and Sr. Looking at the phase shifts calculated by FEFF for these two atoms, their difference was found to be almost π for $k > 7.5$ Å^{-1}. By simulating the RDFs we could show that there is a minimum of the peak height and the apparent distance for a ratio near 1:1. Both for larger and smaller ratios the peak increases and shifts toward larger R values.

The same considerations hold true for the Cu/Ru shell. Here the difference for the phase shifts is exactly π for $k > 7.5$ Å^{-1}. As a result, the interfering backscattering contributions of Cu and Ru lead to a strong decrease of the peak height. This effect is most evident when comparing Figure 4b ($y = 0.6$) and Figure 7b ($y = 0.8$).

Distances calculated from the XAS and XRD data agree quite well for the Cu/Ru shell. Again the former are smaller by about 0.02 Å. No significant difference between the Ru−Ru and Ru−Cu distances could be detected. The coordination numbers reveal an almost statistical arrangement of Cu and Ru on the B cation positions. Still, the Cu content is slightly larger than expected.

For the three samples with $y = 0.6$ the Cu/Ru ratio should be equal. Actually some small differences of N could be detected. This indicates that an increasing La content leads to a slight enrichment of Cu in the Ru neighborhood.

For the oxygen shell at $(1,^1/_2,0)$ coordination numbers varied between 2 and 11. This fact shows that the importance of this scattering path changes dramatically for the different compounds.

Considering the second La/Sr shell the distances calculated by WinXAS are about 0.02 Å smaller than the ones found by Rietveld refinements. Again the coordination numbers show an excellent agreement with those calculated for a statistical contribution.

To verify our results we also have performed XAS measurements at the Cu−K edge for the same samples as above.

The results for both edges should be consistent, i.e., the distances must be the same and the coordination numbers should reveal a random arrangement for the different atom species.

Due to the experimental setup at the E4 beamline at HASYLAB measurements had to be carried out at room temperature. As a result, possible deviations of the distances might simply be caused by thermal expansion.

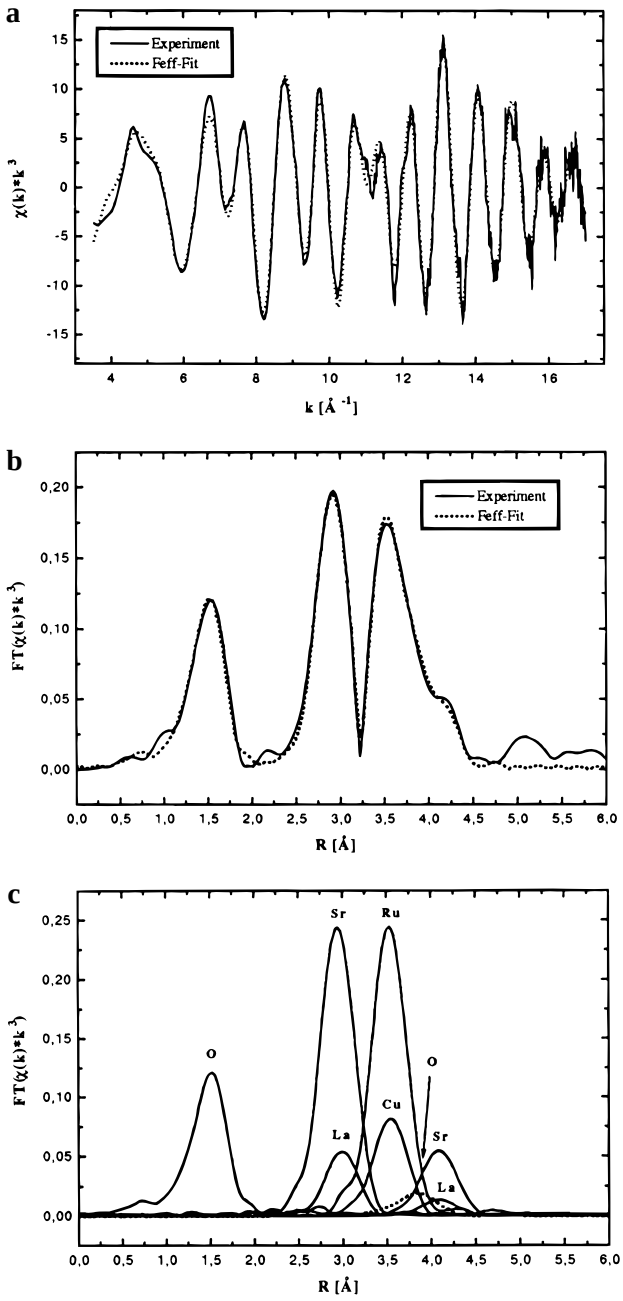

Figure 7. (a) Extracted $\chi(k)k^3$ and its simulation using the parameters given in Table 3 for the Ru−K edge EXAFS of the sample $La_{0.2}Sr_{1.8}Cu_{0.2}Ru_{0.8}O_{4-\delta}$. (b) The corresponding Fourier transform and its simulation for the same sample. (c) Contribution of the different atom species to the simulated Fourier transform in Figure 7b. Note that the interference between the backscattering contributions leads to a decrease of the peak heights both for the Cu/Ru and La/Sr shells.

We have used $La_{1.9}Sr_{0.1}CuO_4$ as reference material to determine S_0^2 and the Debye−Waller factors for O, La, and Cu. σ(Sr) was calculated using $La_{0.08}Sr_{1.92}Cu_{0.2}Ru_{0.8}O_{4-\delta}$ as reference material. For both compounds, we have assumed that the error due to the small amount of Sr and La, respectively, is negligible.

Again the oxygen shell was fitted separately. Except for $x = 1.92$ and $y = 0.6$, the second La/Sr peak was too small to be fitted. So this shell was omitted for all other samples. The results of our calculations are summarized in Table 3.

For the oxygen shell it was found that the distances are larger than the ones calculated from the Ru−K data. This might be due to the higher temperature (*RT* vs 77 K). The coordination number decreases with increasing ratio $x/2y$ as expected from

TABLE 3: Refined Structure Parameters for the Ru−K and Cu−K EXAFS Analysis of the System $La_{2-x}Sr_xCu_{1-y}Ru_yO_{4-\delta}$[a]

	E_0	S_0^2	atom	N	R [Å]	σ [Å^2]		E_0	S_0^2	atom	N	R [Å]	σ [Å^2]
			$x = 2$ and $y = 1$							$x = 1.36$ and $y = 0.6$			
Ru−K	−3.04 (35)	0.85 (5)	O	[6]	1.93 (2)	0.0041 (2)	Ru−K	−0.44 (3)	[0.85]	O	6.18 (36)	1.93 (1)	[0.0041]
	−2.76 (16)	0.73 (4)	Sr	[8]	3.29 (1)	0.0028 (1)		−2.80 (16)	[0.73]	La 2.56	2.66 (31)	3.30 (2)	[0.0028]
			Ru	[8]	3.86 (1)	0.0017 (1)				Sr 5.44	5.34 (31)	3.30 (2)	[0.0028]
			O	[16]	[4.33]	0.0052 (3)				Cu 3.2	4.09 (23)	3.85 (2)	[0.0017]
			Sr	[4]	4.48 (1)	0.0031 (2)				Ru 4.8	3.91 (23)	3.85 (2)	[0.0017]
										O	10.56 (61)	[4.34]	[0.0052]
			$x = 1.8$ and $y = 0.8$							La 1.28	1.31 (16)	4.53 (3)	[0.0031]
Ru−K	−1.42 (10)	[0.85]	O	5.86 (33)	1.94 (1)	[0.0041]				Sr 2.72	2.69 (16)	4.53 (3)	[0.0031]
	−4.67 (27)	[0.73]	La 0.8	1.16 (40)	3.28 (2)	[0.0028]	Cu−K	−0.25 (20)	[0.52]	O	6.17 (36)	1.94 (2)	[0.0039]
			Sr 7.2	6.84 (40)	3.29 (2)	[0.0028]		−6.30 (41)	[0.52]	La 2.56	2.36 (33)	3.25 (1)	[0.0051]
			Cu 1.6	2.25 (33)	3.89 (1)	[0.0017]				Sr 5.44	5.64 (33)	3.25 (1)	[0.0083]
			Ru 6.4	5.75 (33)	3.88 (1)	[0.0017]				Cu 3.2	1.80 (36)	3.89 (1)	[0.0029]
			O	10.03 (71)	[4.36]	[0.0052]				Ru 4.8	6.20 (36)	3.89 (1)	[0.0029]
			La 0.4	0.64 (19)	4.47 (3)	[0.0031]							
			Sr 3.6	3.36 (19)	4.47 (3)	[0.0031]				$x = 1.4$ and $y = 0.4$			
Cu−K	−3.90 (23)	[0.52]	O	5.62 (32)	1.98 (2)	[0.0039]	Ru−K	0.84 (5)	[0.85]	O	5.81 (28)	1.93 (1)	[0.0041]
	−7.12 (41)	[0.52]	La 0.8	0.33 (44)	3.23 (1)	[0.0051]		−1.66 (10)	[0.73]	Sr 2.4	2.73 (17)	3.28 (2)	[0.0028]
			Sr 7.2	7.67 (44)	3.25 (1)	[0.0083]				Sr 5.6	5.27 (17)	3.29 (1)	[0.0028]
			Cu 1.6	1.40 (38)	3.89 (1)	[0.0029]				Cu 4.8	4.80 (27)	3.88 (1)	[0.0017]
			Ru 6.4	6.60 (38)	3.90 (1)	[0.0029]				Ru 3.2	3.20 (27)	3.88 (1)	[0.0017]
										O	2.05 (70)	[4.33]	[0.0052]
			$x = 1.92$ and $y = 0.6$							La 1.2	1.56 (20)	4.54 (2)	[0.0031]
Ru−K	1.10 (6)	[0.85]	O	6.14 (35)	1.94 (1)	[0.0041]				Sr 2.8	2.44 (20)	4.54 (2)	[0.0031]
	−3.00 (17)	[0.73]	La 0.32	1.12 (40)	3.30 (2)	[0.0028]	Cu−K	−2.03 (12)	[0.52]	O	4.63 (27)	1.93 (4)	[0.0039]
			Sr 7.68	6.88 (40)	3.30 (1)	[0.0028]		−2.63 (24)	[0.52]	La 2.4	2.85 (30)	3.28 (3)	[0.0051]
			Cu 3.2	3.60 (25)	3.90 (1)	[0.0017]				Sr 5.6	5.15 (30)	3.28 (3)	[0.0083]
			Ru 4.8	4.40 (25)	3.89 (1)	[0.0017]				Cu 4.8	4.33 (25)	3.88 (2)	[0.0029]
			O	4.82 (28)	[4.37]	[0.0052]				Ru 3.2	3.67 (25)	3.90 (2)	[0.0029]
			La 0.16	0.79 (19)	4.44 (2)	[0.0031]							
			Sr 3.84	3.21 (19)	4.44 (2)	[0.0031]				$x = 1.2$ and $y = 0.2$			
Cu−K	−4.33 (25)	[0.52]	O	4.87 (28)	1.96 (4)	[0.0039]	Cu−K	−1.29 (10)	[0.52]	O	4.59 (27)	1.91 (4)	[0.0039]
	−6.00 (57)	[0.52]	Sr	[8]	3.23 (1)	0.0083 (1)		−2.27 (19)	[0.52]	La 3.2	3.05 (29)	3.23 (2)	[0.0051]
			Cu 3.2	2.50 (28)	3.89 (2)	[0.0029]				Sr 4.8	4.95 (29)	3.23 (2)	[0.0083]
			Ru 4.8	5.50 (28)	3.90 (3)	[0.0029]				Cu 6.4	5.00 (30)	3.84 (1)	[0.0029]
			Sr	[4]	4.42 (1)	0.0072 (2)				Ru 1.6	3.00 (30)	3.85 (1)	[0.0029]
			$x = 1.6$ and $y = 0.6$							$x = 0.1$ and $y = 0$			
Ru−K	−1.35 (8)	[0.85]	O	6.34 (37)	1.92 (1)	[0.0041]	Cu−K	7.05 (41)	0.52 (3)	O	[6]	1.92 (2)	0.0039 (4)
	−3.47 (20)	[0.73]	La 1.6	1.93 (35)	3.29 (2)	[0.0028]		−4.10 (24)	0.52 (3)	La	[8]	3.24 (1)	0.0051 (1)
			Sr 6.4	6.07 (35)	3.30 (2)	[0.0028]				Cu	[8]	3.79 (1)	0.0029 (1)
			Cu 3.2	3.95 (23)	3.89 (3)	[0.0017]							
			Ru 4.8	4.05 (23)	3.88 (1)	[0.0017]							
			O	7.43 (43)	[4.37]	[0.0052]							
			La 0.8	0.88 (27)	4.48 (2)	[0.0031]							
			Sr 3.2	3.12 (27)	4.48 (2)	[0.0031]							
Cu−K	−5.59 (32)	[0.52]	O	5.24 (28)	1.95 (4)	[0.0039]							
	−4.07 (50)	[0.52]	La 1.6	1.60 (40)	3.27 (3)	[0.0051]							
			Sr 6.4	6.40 (40)	3.25 (2)	[0.0083]							
			Cu 3.2	2.09 (34)	3.89 (2)	[0.0029]							
			Ru 4.8	5.91 (34)	3.92 (1)	[0.0029]							

[a] N = coordination number. R = bond length. σ = Debye−Waller factor. Fixed values are given in square brackets. The values listed in the atom column are theoretical coordination numbers assuming a statistical contribution of the A and B cations.

our thermogravimetric results. This fact proves that oxygen vacancies are located exclusively in the coordination sphere of copper. For $6 > N > 5$, the Cu surrounding consists of (slightly elongated) octahedra and tetragonal pyramids. Looking at Table 3 it can be seen that we found values of N even smaller than 5. This means that a part of the copper ions is coordinated in a quadratic planar way.

For the first La/Sr shell the distances calculated from the Cu−K data are approximately 0.05 Å smaller than those from the Ru−K XAS. This is quite surprising as the higher temperature for the former measurements is expected to lead to larger distances. As already discussed for the Ru−K measurements, the distances Cu−La and Cu−Sr are equal for all samples. This indicates that there are two characteristic distances, namely, Ru−La/Sr (3.30 Å) and Cu−La/Sr (3.25 Å). As a result the cube of A cations around copper is significantly smaller than the one around Ru. Nevertheless, we cannot exclude that the different distances are an artifact due to incorrect theoretical phase shifts.

Considering the coordination numbers we found a random distribution of the different A cation species. The values for N excellently agree with the ones obtained from the Ru−K EXAFS.

The distance Cu−Cu turned out to be equal to the distance Cu−Ru for all compounds. The values agree well both with the Ru−K EXAFS and the XRD results.

For most of the samples the coordination numbers reveal an almost statistical distribution of the B cations. For the three samples with $y = 0.6$ the ratio Ru:Cu increases with an increasing La content. This confirms our results for the Ru−K EXAFS where an increasing La content was found to lead to an enrichment of Cu in the Ru neighborhood. For this reason we conclude that a larger La content leads to a transition from a statistical distribution (Figure 2b) to an ordered arrangement of the B cations such as the one displayed in Figure 2c.

Conclusion

EXAFS was found to be an extremely powerful tool for the investigation of the layered perovskite system $La_{2-x}Sr_xCu_{1-y}Ru_yO_{4-\delta}$.

We were able to achieve consistent results both from the Ru−K and Cu−K X-ray absorption edge measurements. This agreement confirms the high reliability of our results.

The interatomic distances derived from EXAFS and Rietveld refinement calculations of XRD data agree quite well. Nevertheless, the former are usually smaller by approximately 0.02 Å. This indicates that the accuracy of the theoretical phase shifts still can be improved.

The distances between all possible combinations of B cations (Ru−Ru, Ru−Cu, and Cu−Cu) were found to be equal within the usual experimental error of ±1%. The same holds true for the distances (Ru−La, Ru−Sr) and (Cu−La, Cu−Sr). We found that the distance Cu−La/Sr is smaller than the distance Ru−La/Sr for all samples. This fact indicates that the size of the A cation cube is only influenced by the kind of the B cation in its center, while it is independent of the nature of the cations at its edges.

The calculated coordination numbers clearly reveal that La and Sr are distributed statistically on the A cation position. For the B cations the situation is more complicated. Generally spoken Ru and Cu are also statistically distributed. Still we found that an increasing La content leads to an enrichment of Cu in the Ru surrounding and vice versa. This can be seen as a hint for the occurrence of an short range ordering within the BO_2 planes.

The thermogravimetrically detected oxygen vacancies were found to be located exclusively in the copper surrounding while Ru remains in an octahedral coordination sphere.

The fact that we have found coordination numbers less than 5 reveals that the system $La_{2-x}Sr_xCu_{1-y}Ru_yO_{4-\delta}$ avoids very high oxidation states not only by the formation of CuO_5-pyramids but also by a partial formation of CuO_4-square planes.

This information can be most useful for the interpretation of electrical and magnetical experiments.

By comparing X-ray diffraction and EXAFS, it can be stated that the former yields distances with a much higher accuracy while the latter gives detailed element specific information about the local environment. Therefore, both methods complement one another in an ideal way.

Acknowledgments. We wish to thank Dr. K. H. Klaska at the Institute of Mineralogy and Petrography, University of Hamburg, for performing the XRD measurements and the HASYLAB for allocating beamtime.

References and Notes

(1) Ebbinghaus, S.; Reller, A. *Solid State Ionics* **1997**, in press.

(2) Frahm, R. *Instrum. Methods Phys. Res.* **1988**, *A270*, 578.

(3) Ressler, T. *J. Phys. IV (France)* **1997**, *7*, C2−269.

(4) Rehr, J. J.; Mustre de Leon, J.; Zabinsky, S. I.; Albers, R. C. *J. Am. Chem. Soc.* **1991**, *113*, 5135.

(5) Young, R. A.; Sakthivel, A.; Moss, T. S.; Paiva-Santos, C. O. *User's Guide to Program DBWS-9411 for Rietveld Analysis of X-ray and Neutron Powder Diffraction Patterns*; 1994.

(6) Teo, B. K. *EXAFS: Basic Principles and Data Analysis*; Springer: Berlin, 1986; Chapter 2.